*Article*

# Nonlinear Modeling and Coordinate Optimization of Semi-Active Energy Regenerative Suspension with Electro-Hydraulic Actuator

**Farong Kou [1,*], Jiafeng Du [1], Zhe Wang [1], Dong Li [1] and Jianan Xu [1]**

1 College of Mechanical Engineering, Xi'an University of Science and Technology, Xi'an 710054, China

* Correspondence: kfr2000@163.com or koufarong@xust.edu.cn

**Abstract:** In order to coordinate the damping performance and energy regenerative performance of energy regenerative suspension, this paper proposes a structure of vehicle semi-active energy regenerative suspension with electro-hydraulic actuator (EHA). In light of the proposed concept, a specific energy regenerative scheme is designed and the mechanical properties test is carried out. Based on the test results, the parameter identification for the system model is conducted using recursive least squares algorithm. On the basis of system principle, the nonlinear model of the semi-active energy regenerative suspension with EHA is built. Meanwhile, LQG control strategy of the system is designed. And then the influence of the main parameters of EHA on the damping performance and energy regenerative performance of suspension is analyzed. Finally, the main parameters of EHA actuator are optimized via genetic algorithm. The test results show that when sinusoidal is input at the frequency of 2Hz and the amplitude of 30mm, the spring mass acceleration RMS value of optimized EHA semi-active energy regenerative suspension is reduced by 22.23% and energy regenerative power RMS value is increased by 40.51%, which means while meeting the requirements of certain vehicle ride comfort and driving safety, energy regenerative performance is improved significantly.

**Keywords**: semi-active suspension; feed energy; parameter optimization; genetic algorithm

---

## 1. Introduction

Suspension system is a key component of the vehicle chassis system, its performance directly determines the ride comfort, operational stability and driving safety of vehicle. The performance of traditional passive suspension without adjustable parameters is difficult to meet the higher requirements[1-2]. With the application of sensor technology and control technology, controllable suspension with superior performance attracts more and more attention. Although the traditional controllable suspension can realize the real-time adjustment of the suspension performance, it is limited by its high cost and high energy consumption[3-5].

The type of energy regenerative active suspension raised provided a method to solve the above mentioned problems, that is, through the regenerative of the vibration energy caused by the uneven road surface, the energy dissipated by the energy dissipation of shock absorber can be converted into the electric energy that can be recycled to reduce the energy consumption of the active suspension[6-8]. At present, the research on energy regenerative suspension is mainly focused on how to improve the efficiency of energy regenerative, while ignoring the original design of the suspension and lacking the coordination analysis of the suspension system damping performance and energy regenerative performance[9-11].

Lei Zuo et al.[12-13] designed a type of gear rack energy regenerative suspension, carried out theoretical and experimental studies, and analyzed the relationship between vehicle ride comfort and handling stability and suspension energy regenerative performance. The bench test results show that the suspension is effective for vibration attenuation and the vibration energy regenerative efficiency is improved. Yu Fan et al.[14] integrated the ball screw and the DC motor into a suspension, optimized the damping characteristics of the suspension and recovered the vibration energy. Yu Changmiao et al.[15] put forward the gear rack energy regenerative suspension, and set up a clutch mechanism in the motor and the gear rack mechanism. The simulation analysis results show that it can regenerate energy at the same time basically meeting the requirements of the vehicle ride comfort and handling stability.

On the basis of the above research, this paper proposes a structure of vehicle semi-active energy regenerative suspension with EHA in Section 2. A quarter-car model with two degrees of freedom is built in Section 3.1; then the mechanical properties test is carried out, and according to the test results, we perform the parameter identification for the system model using recursive least squares algorithm in Section 3.2; and the nonlinear model of the semi-active energy regenerative suspension with EHA is established in Section 3.3. In Section 4, LQG control strategy of semi-active energy regenerative suspension with EHA is designed. Moreover, the influences of the main parameters of EHA on the damping performance and energy regenerative performance of suspension are analyzed in Section 5.1;then the main parameters of EHA are optimized via genetic algorithm in Section 5.2, and the bench test is carried out in Section 5.4. Finally, conclusions are summarized in Section 6.

## 2. Structure and principle of semi-active energy regenerative suspension with EHA

The basic structure of semi-active energy regenerative suspension system with EHA is shown in Figure 1. The system is mainly composed of spiral spring, hydraulic cylinder, hydraulic motor, brushless DC motor, DSP controller, composite energy recovery device, digital potentiometer and the corresponding sensor. The hydraulic cylinder use double pole double acting symmetrical hydraulic cylinder; The hydraulic motor use gear motor that can carry out positive inversion; The brushless DC generator use permanent magnet brushless DC generator[16].

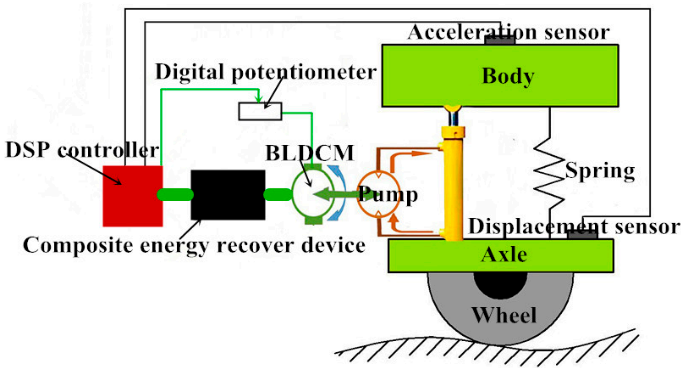


**Figure 1.** The structure of semi-active energy regenerative suspension with EHA.

When the vehicle is running, the hydraulic cylinder moves with the body vibration and pushes hydraulic oil to drive the hydraulic motor to rotate, the output shaft of the hydraulic motor drives the coaxial brushless DC generator by coupling, the generated electrical energy is recovered and stored by a composite energy recovery device to realize energy regenerative of EHA energy regenerative suspension. At the same time, the sensor sends the signal of the vehicle operation condition to the controller. According to the control strategy, the controller changes the external load resistance value of brushless DC motor by adjusting the value of digital potentiometer. Therefore, the electromagnetic torque of the motor can be changed, and the damping force of the hydraulic cylinder can be controlled to realize the control function of the EHA semi-active suspension.

Peer-reviewed version available at Algorithms 2018, 11, 12; doi:10.3390/a11020012



The composite energy recovery device is shown in Figure 2. The device is mainly composed of three-phase rectifier, filter circuit, boost module 1, boost module 2, MOSFET A, MOSFET B, voltage equalizing circuit, super capacitor group, voltage sensor, DSP controller, voltage stabilizing circuit, diode and storage battery. Among them, the super capacitor group consists of 4 2.7V100F super capacitor series, in which the voltage is 10.8V, the capacity is 25F and the optimal charging voltage is 9-10V. The boost module 1 boosts to 9V for super capacitor charging. Referring to the vehicle battery, the lead-acid battery used is 12V8AH, in which the optimal charging voltage is 14.40.2V. The booster module 2 boosts to 14.4V for charging the battery after voltage stabilizing circuit. In order to prevent the battery from over charging of the super capacitor, a unidirectional conducting diode is connected in series between the voltage stabilizing circuit and the storage battery.

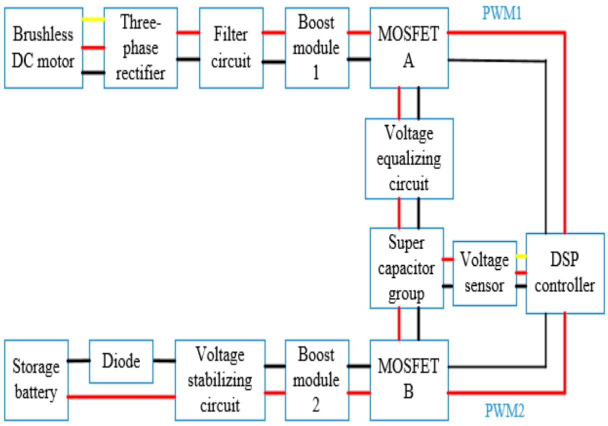


**Figure 2.** Illustrative diagram of the complex energy recovery device.

The specific working process of the composite energy recovery device: The voltage sensor connected in parallel at both ends of the super capacitor group is detected in real time by the super capacitor group's voltage signal which is collected to the DSP controller by the A/D sampling module of the DSP controller. When the voltage at both ends of the super capacitor group is detected to reach 4V, the DSP controller outputs two PWM signals, one output PWM1 is higher and it drives the MOSFET switch A to open. The other one output PWM2 is lower and it drives the MOSFET switch B to close. At this moment, the super capacitor group is in charge status and the three-phase alternating current generated by the brushless DC motor through a three-phase rectifier bridge and a filter circuit becomes a stable DC voltage that is boosted to 9V by the boost module 1. The super capacitor group is steadily charged by 9V's voltage through the MOSFET switch A and the equalizing circuit. When the voltage at both ends of the super capacitor group is detected to reach 9V, the DSP controller outputs two PWM signals, one output PWM2 is high and it drives the MOSFET switch B to open. The other one output PWM1 is low and it drives the MOSFET switch A to close. At this moment, the super capacitor group is in discharge status and the output voltage of the super capacitor grope is boosted to 14.4V by the boost module 2. The storage battery is steadily charged by 14.4V's voltage through voltage stabilizing circuit. In order to prevent over discharge of the super capacitor group, the minimum discharge voltage of the super capacitor group is set at 4V, that is, when the voltage sensor detects that the voltage between the two ends of the super capacitor group reaches 4V, the mode is converted, and the whole system performs cyclic charge and discharge.

Preprints (www.preprints.org) | NOT PEER-REVIEWED | Posted: 19 December 2017 doi:10.20944/preprints201712.0129.v1

Peer-reviewed version available at Algorithms 2018, 11, 12; doi:10.3390/a11020012



## 3. Nonlinear modeling of semi-active energy regenerative suspension with EHA

### *3.1. Dynamic model of 2 degrees of freedom suspension system for 1/4 vehicle*

In this paper, a quarter-car model with two degrees of freedom was exactly established[17], which is shown in Figure 3.

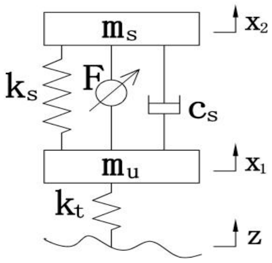


**Figure 3.** The schematic diagram of a quarter-car model.

According to figure 3, the equations of motion are obtained by using Newtons laws of motion:

$$\begin{cases} m_s\ddot{x}_2 + k_s(x_2 - x_1) + c_s(\dot{x}_2 - \dot{x}_1) = F \\ m_u\ddot{x}_1 - k_s(x_2 - x_1) - c_s(\dot{x}_2 - \dot{x}_1) + k_t(x_1 - z) = -F \end{cases} \tag{1}$$

The state vector and output vector are selected as follows:

$$\boldsymbol{X} = \begin{bmatrix} x_2 - x_1 & \dot{x}_2 & x_1 - z & \dot{x}_1 \end{bmatrix}^{\mathrm{T}}$$

$$\boldsymbol{Y} = \begin{bmatrix} \ddot{x}_2 & x_2 - x_1 & k_t(x_1 - z) & \dot{x}_1 \end{bmatrix}^{\mathrm{T}}$$

where $\ddot{x}_2$ is sprung mass acceleration, $x_2 - x_1$ is suspension deflection response, $k_t(x_1 - x_0)$ is tire load response, and $\dot{z}(t)$ is speed excitation of road input. In this way, the state equation of suspension can be obtained as follows:

$$\begin{cases} \dot{\boldsymbol{X}} = \boldsymbol{AX} + \boldsymbol{BU} \\ \boldsymbol{Y} = \boldsymbol{CX} + \boldsymbol{DU} \end{cases} \tag{2}$$

where $\boldsymbol{A}$ is state matrix, $\boldsymbol{B}$ is input matrix, $\boldsymbol{C}$ is output matrix, and $\boldsymbol{D}$ is transfer matrix. When the control input force $F$ is 0, it becomes passive suspension.

$$\boldsymbol{A} = \begin{bmatrix} 0 & 1 & 0 & -1 \\ -\dfrac{k_s}{m_s} & -\dfrac{c_s}{m_s} & 0 & \dfrac{c_s}{m_s} \\ 0 & 0 & 0 & 1 \\ \dfrac{k_s}{m_u} & \dfrac{c_s}{m_u} & -\dfrac{k_t}{m_u} & -\dfrac{c_s}{m_u} \end{bmatrix} \qquad \boldsymbol{B} = \begin{bmatrix} 0 & 0 \\ 0 & \dfrac{1}{m_s} \\ -1 & 0 \\ 0 & -\dfrac{1}{m_u} \end{bmatrix}$$

$$\boldsymbol{C} = \begin{bmatrix} -\dfrac{k_s}{m_s} & -\dfrac{c_s}{m_s} & 0 & \dfrac{c_s}{m_s} \\ 1 & 0 & 0 & 0 \\ 0 & 0 & k_t & 0 \\ 0 & 0 & 0 & 1 \end{bmatrix} \qquad \boldsymbol{D} = \begin{bmatrix} 0 & \dfrac{1}{m_s} \\ 0 & 0 \\ 0 & 0 \\ 0 & 0 \end{bmatrix} \qquad \boldsymbol{U} = \begin{pmatrix} \dot{z} \\ F \end{pmatrix}$$

The road surface input model adopts a filtered white noise [18] as follows:

$$\dot{z}(t) = -2\pi f_0 z(t) + 2\pi\sqrt{G_0 u}\,\omega(t) \tag{3}$$

where $z$ is the input displacement of the road, $G_0$ is road irregularities coefficient, $f_0$ is lower cutoff frequency, $u_0$ is vehicle speed, and $\omega(t)$ is unit white noise.

Peer-reviewed version available at Algorithms 2018, 11, 12; doi:10.3390/a11020012



*3.2. Parameter identification of nonlinear model*

In order to provide experimental sample data for the model parameter identification, the physical prototype of EHA actuator is developed, and according to the national standards of QC/T545-1999 "Test method for automobile telescopic shock absorber", the force characteristics test of EHA semi-active suspension system is carried out on the ES-6-230 numerical control hydraulic vibration table, as shown in Figure 4. In the experiment, the vibration table input excitation uses sinusoidal input at the frequency of 1Hz and the amplitude of 30mm. LTR-1 pull pressure sensor is used to collect suspension output force signal in the passive state, and the change of the suspension output force with time is shown in Figure 5. In order to eliminate the influence of initial conditions on the test results, the sampling time starts from 5s.

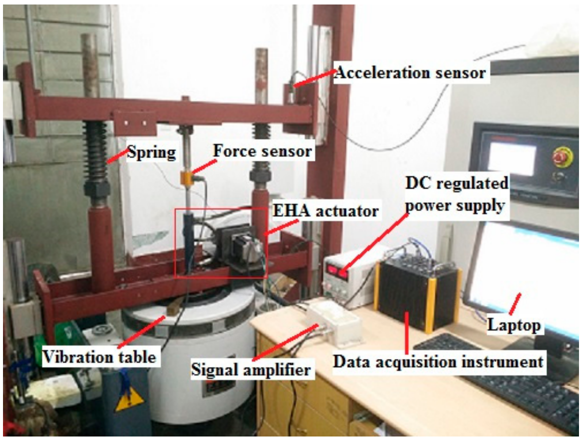


**Figure 4.** Force characteristic test of EHA semi-active suspension system.

The parameters of the nonlinear model are continuously approximated by the least squares method based on the experimental data, and the objective function of the algorithm is expressed as:

$$\{k_s, c_s\} = \arg\min_{k_s, c_s} \left\| F_c(k_s, c_s) - F_e \right\|_2^2 \tag{4}$$

where $k_s$ is equivalent spring stiffness, $c_s$ is inherent damping coefficient of the system, $F_c$ is theoretical model value, and $F_e$ is actual test value.

Through the identification of the parameters, the equivalent spring stiffness $k_s$ of the EHA semi-active suspension system is 13000 $\mathrm{N/m}$, and the inherent damping coefficient $c_s$ is 500 $\mathrm{N \cdot m/s}$. The above parameters are introduced into the two degree of freedom suspension dynamics model of the 1/4 vehicle, and the simulation results of the EHA actuator output force are compared with the test results, as shown in Figure 5.

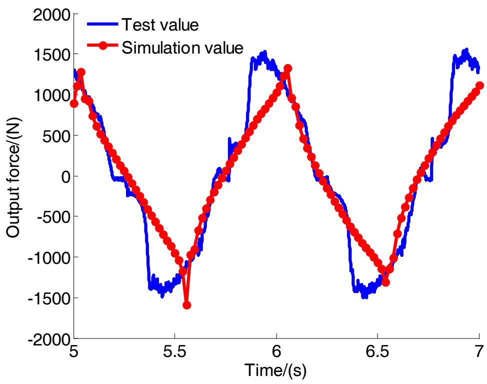


**Figure 5.** Comparison of simulation and experimental results of output force.

Figure 5 shows the output force of the EHA actuator obtained by parameter identification is in good agreement with the actual output force, which indicates the established dynamic model of 2 degrees of freedom suspension system for 1/4 vehicle is accurate, and the adopted method of model parameter identification is feasible and effective.

### 3.3. Mathematical model of semi-active energy regenerative suspension with EHA

When the mathematical model of the EHA actuator is established, the friction between the piston, the cylinder wall and the internal leakage of the system are ignored. Thus the damping force generated by the hydraulic cylinder can be expressed as:

$$F = \Delta P \cdot A \tag{5}$$

where $\Delta P$ is pressure drop between upper and lower surface of piston in hydraulic cylinder, and $A$ is effective piston area.

Taking into account the hydraulic pipeline's pressure loss which includes the pressure loss along the path and the local pressure loss[19].

Among them, the pressure loss along the path of the hydraulic pipeline in the system is expressed as:

$$\Delta P_{\lambda} = \lambda \frac{l}{d} \left(\frac{\rho v^2}{2}\right) \tag{6}$$

where $\lambda$ is along resistance coefficient, $l$ is length of hydraulic pipe, $d$ is diameter of hydraulic pipe, $\rho$ is hydraulic oil density, and $v$ is oil flow rate in pipeline.

The local pressure loss of the hydraulic pipeline in the system is expressed as:

$$\Delta P_{\zeta} = \zeta \frac{\rho v^2}{2} \tag{7}$$

where $\zeta$ is local resistance coefficient.

It can be seen that the total pressure loss of the hydraulic pipeline in the system can be obtained as follows:

$$\Delta P_g = \Delta P_{\lambda} + \Delta P_{\zeta} = \left(\lambda \frac{l}{d} + \zeta\right) \frac{\rho v^2}{2} \tag{8}$$

According to the continuity equation of liquid flow, which is given by:

$$Q_d = A \cdot v_g = \frac{\pi d^2}{4} v \tag{9}$$

where $Q_d$ is flow of hydraulic motor , and $v_g$ is speed of piston rod.

According to the working principle of semi-active energy regenerative suspension with EHA, it can be seen that under the action of body vibration the oil in the hydraulic cylinder enters the hydraulic motor and drives the hydraulic motor to work, and the output torque of the hydraulic motor drives the generator to generate electricity. At the same time, the angular velocity and output torque of the hydraulic motor meet the following relationships:

$$\omega_0 = \frac{2\pi Q_d}{q} \eta_v \tag{10}$$

$$T_d = \frac{\Delta p_d q}{2\pi} \eta_m \tag{11}$$

Peer-reviewed version available at Algorithms 2018, 11, 12; doi:10.3390/a11020012



where $q$ is hydraulic motor displacement, $\eta_v$ is volumetric efficiency of the hydraulic motor, $\Delta p_d$ is pressure drop between inlet and outlet of the hydraulic motor, and $\eta_m$ is mechanical efficiency of the hydraulic motor.

The generator converts the mechanical energy of the hydraulic motor into electrical energy, so the input torque of the generator is equal to the output torque of the hydraulic motor. Therefore the output voltage $U$ and the output torque $T_g$ of the generator meet the following relationships:

$$U = E - I(r + R) = IR_0 \tag{12}$$

$$T_g = J\ddot{\theta} + k_t I \tag{13}$$

where $E$ is induced electromotive force, $I$ is loop current, $r$ is internal resistance of the generator, $R$ is external load resistance of the generator, $R_0$ is equivalent resistance of energy regenerative circuit, $J$ is the moment of inertia, $\ddot{\theta}$ is angular acceleration of the generator, and $k_t$ is torque constant of the generator.

Among them, the induction electromotive force is expressed as:

$$E = k_e n = \frac{30}{\pi} k_e \omega \tag{14}$$

where $k_e$ is back electromotive force constant of the generator, $n$ is generator rotor speed, and $\omega$ is generator rotor angular velocity.

The hydraulic motor is directly connected with the generator through the coupling, so their angular velocity and torque are equal, which is expressed as $\omega_0 = \omega$ and $T_d = T_g$. If the moment of inertia of the motor is ignored, pressure drop between inlet and outlet of the hydraulic motor can be obtained from Eqs. (9)~(14) as follows:

$$\Delta P_d = \frac{120\pi k_e k_t \eta_v A v_g}{q^2 \eta_m (r + R + R_0)} \tag{15}$$

The pressure balance equation of the whole hydraulic circuit be expressed as:

$$\Delta P = \Delta P_d + \Delta P_g = \frac{120\pi k_e k_t \eta_v A v_g}{q^2 \eta_m (r+R+R_0)} + \left(\lambda \frac{l}{d} + \zeta\right) \frac{8\rho A^2 v_g^2}{\pi^2 d^4} \tag{16}$$

The damping force of the EHA actuator can be obtained by taking Eqs. (16) into Eqs. (14) as follows:

$$F = \frac{120\pi k_e k_t \eta_v A^2 v_g}{q^2 \eta_m (r+R+R_0)} + \left(\lambda \frac{l}{d} + \zeta\right) \frac{8\rho A^3 v_g^2}{\pi^2 d^4} \tag{17}$$

Therefore the equivalent damping coefficient of the EHA actuator can be expressed as:

$$c_{eq} = \frac{120\pi k_e k_t \eta_v A^2}{q^2 \eta_m (r+R+R_0)} + \left(\lambda \frac{l}{d} + \zeta\right) \frac{8\rho A^3 v_g}{\pi^2 d^4} \tag{18}$$

Loop current can be obtained from Eqs. (11), (13) and (15) as follows:

$$I = \frac{60 k_e \eta_v A v_g}{q(r + R + R_0)} + \left(\lambda \frac{l}{d} + \zeta\right) \frac{4\rho q \eta_m A^2 v_g^2}{\pi^3 d^4 k_t} \tag{19}$$

In summary, the instantaneous energy regenerative power can be expressed as:

Peer-reviewed version available at Algorithms 2018, 11, 12; doi:10.3390/a11020012



$$P_{reg} = I^2 R_0 = \left[ \frac{60 k_e \eta_v A v_g}{q(r+R+R_0)} + \left( \lambda \frac{l}{d} + \zeta \right) \frac{4 \rho q \eta_m A^2 v_g^2}{\pi^3 d^4 k_t} \right]^2 R_0 \tag{20}$$

In the traditional passive suspension damper, the dissipated power in the form of heat energy is calculated as:

$$P_{con} = c_s (\dot{x}_2 - \dot{x}_1)^2 \tag{21}$$

where $c_s$ is inherent damping coefficient, and $(\dot{x}_2 - \dot{x}_1)$ is shock absorber velocity.

The energy regenerative efficiency of semi-active suspension is the ratio between the feedback energy and dissipated energy of the passive suspension. Therefore the energy regenerative efficiency $\eta$ is expressed as:

$$\eta = \frac{\int_0^T P_{reg} \mathrm{d}t}{\int_0^T \left[ c_s (\dot{x}_2 - \dot{x}_1)^2 \right] \mathrm{d}t} \tag{22}$$

## 4. The control strategy of semi-active energy regenerative suspension with EHA

The selection principle of switching control critical point to control force of semi-active energy regenerative suspension with EHA.

When $\dot{x}_2 \cdot (\dot{x}_2 - \dot{x}_1) > 0$, the direction of the force applied to the spring mass by the actuator is opposite to movement direction of the spring mass, but it has the same direction as the active control force, so it can change the external load resistance of the actuator to make the actual control output force be equal to the theoretical active control output force. And the theoretical active control output force is determined by the optimal control strategy.

The optimal control objective of semi-active energy regenerative suspension with EHA is to make the car get higher comfort and handling stability, and reflecting in the amount of actual control is to reduce the acceleration of sprung mass and tire dynamic load as much as possible, limit the range of suspension dynamic deflection, and reduce the possibility of Suspension impact block. At the same time, don't consume too much energy[20]. Based on the above considerations, the performance index function of semi-active suspension output regulator can be written as follows:

$$J = \int_0^\infty \left[ q_1 \ddot{x}_2^2 + q_2 (x_2 - x_1)^2 + q_3 (x_1 - z)^2 + r F^2 \right] \mathrm{d}t \tag{23}$$

where $q_1$ is weighting coefficient of acceleration, $q_2$ is weighting coefficient of suspension dynamic deflection, $q_3$ is weighting coefficient of tire dynamic deformation, and $r$ is weighting coefficient of energy consumption.

The above optimization index is expressed in matrix as:

$$\boldsymbol{J} = \int_0^\infty \left[ \boldsymbol{Y}^{\mathrm{T}} \boldsymbol{q} \boldsymbol{Y} + \boldsymbol{F}^{\mathrm{T}} \boldsymbol{r} \boldsymbol{F} \right] \mathrm{d}\boldsymbol{t} \tag{24}$$

where $q$ is expressed as:

$$\boldsymbol{q} = \begin{bmatrix} q_1 & 0 & 0 \\ 0 & q_2 & 0 \\ 0 & 0 & q_3 \end{bmatrix}$$

Generally, the output regulator problem is converted to a state regulator problem. Taking the output equation $\boldsymbol{Y} = \boldsymbol{CX} + \boldsymbol{DU}$ into equation (24), quadratic performance index is given by:

Preprints (www.preprints.org) | NOT PEER-REVIEWED | Posted: 19 December 2017 doi:10.20944/preprints201712.0129.v1

Peer-reviewed version available at Algorithms 2018, 11, 12; doi:10.3390/a11020012



$$J=\int_0^{\infty}\left[X^{T}QX+2X^{T}NF+F^{T}RF\right]dt \tag{25}$$

where $Q$ is positive semidefinite symmetric weighting matrices of state variables, $N$ is weighted matrix of two kinds of variables, and $R$ is positive definite symmetric weighting matrix of control variables. Among them, $Q=C^{T}qC, N=C^{T}qD, R=r+D^{T}qD$.

The optimal control force $F$ which serves for performance index $J$ to be minimized is existent and unique, it can be expressed as:

$$F=-KX=-(B^{T}P+N^{T})X \tag{26}$$

where $P$ is a symmetric positive definite solution of Riccati matrix equation. It meets the following equation:

$$PA+A^{T}P-(PB+N)R^{1}(B^{T}P+N^{T})+Q=0 \tag{27}$$

The selection of the weighting factors in the performance index of the optimal control depends on the practical experience. After repeated trial, the following options can be made: $q_1=1.2\times10^5$, $q_2=1.65\times10^8$, $q_3=9.5\times10^9$, $r=1$.

In order to obtain feedback gain matrix $K$, using the LQR function provided by Matlab software, the basic format is expressed as:

$$(K,S,E)=\mathrm{LQR}(A,B,Q,R,N) \tag{28}$$

where $S$ is solution of Riccati equation, and $E$ is system eigenvalue.

When $\dot{x}_2\cdot(\dot{x}_2-\dot{x}_1)<0$, the direction of the force applied to the spring mass by the actuator has the same direction as movement direction of the spring mass, but it is opposite to that of the active control force. In order to minimize this difference, at this moment the damping force which is theoretically required to output from the suspension is zero, but the actual output force is the inherent viscous damping force of the system, and its true value is still determined by formula (17). At the same time, the motor load resistance is zero.

## 5. Parameter optimization of semi-active energy regenerative suspension with EHA

### *5.1. Parameter sensitivity analysis*

In order to coordinate the damping performance and energy regenerative performance of semi-active energy regenerative suspension with EHA and improve the energy regenerative performance under the condition of satisfying the requirement of damping performance, the influence of the EHA actuator's parametric variation on the damping performance and energy regenerative performance of suspension is analyzed. The EHA actuator is mainly composed of hydraulic cylinder, hydraulic motor, and brushless DC generator. According to the modeling process, it can be known that the main parameters of the EHA actuator are: the effective area of the hydraulic cylinder piston $A$, the displacement of the hydraulic motor $q$, and back electromotive force constant of the generator $k_e$. Based on the initial simulation parameters value of EHA actuator and 20% of the initial simulation parameters value of the EHA actuator for the change interval, the influence of the three main parameters variation of the EHA actuator on the damping performance and energy regenerative performance of semi-active energy regenerative suspension with EHA is investigated. Among them, the damping performance takes spring mass acceleration and tire dynamic load as evaluation indicator, and energy regenerative performance takes energy regenerative power and energy regenerative efficiency as evaluation indicator. The influence of the main parameters of the EHA actuator on the performance evaluation indicators is shown in Figure 6 ~ Figure 8 respectively.

Preprints (www.preprints.org) | NOT PEER-REVIEWED | Posted: 19 December 2017 doi:10.20944/preprints201712.0129.v1

Peer-reviewed version available at Algorithms 2018, 11, 12; doi:10.3390/a11020012



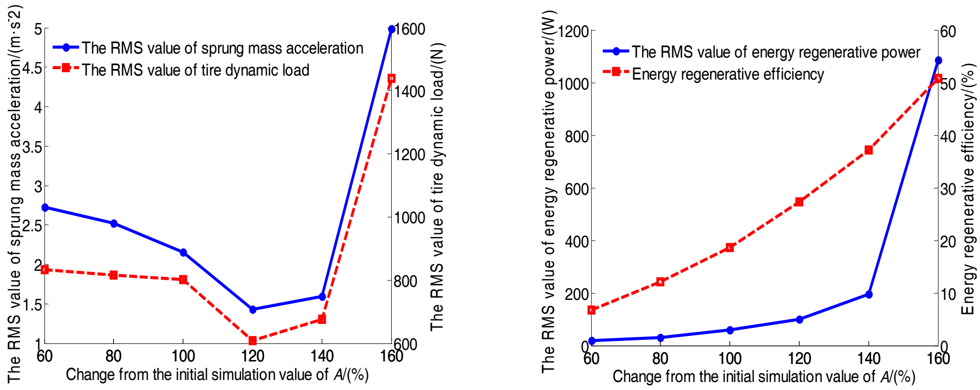


(**a**) (**b**)

**Figure 6.** Influence of the effective area of hydraulic cylinder piston on evaluation indicators: (**a**) Influence of the effective area of hydraulic cylinder piston on the damping performance; (**b**) Influence of the effective area of hydraulic cylinder piston on energy regenerative performance.

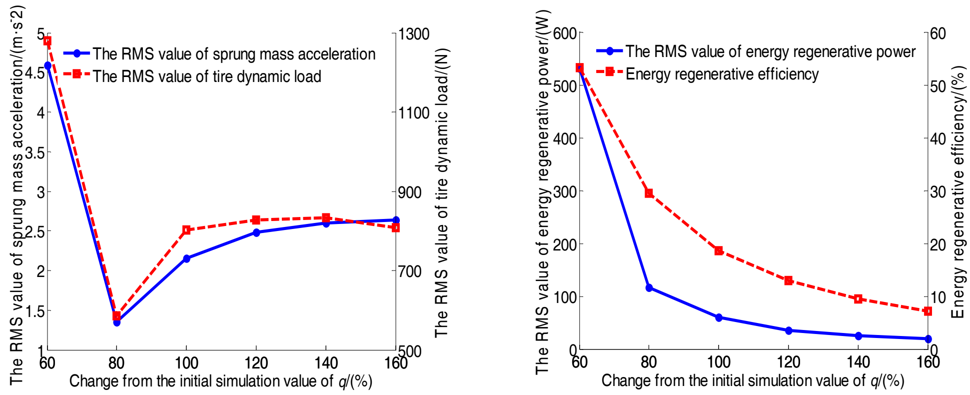


(**a**) (**b**)

**Figure 7.** Influence of the displacement of the hydraulic motor on evaluation indicators: (**a**) Influence of the displacement of the hydraulic motor on the damping performance; (**b**) Influence of the displacement of the hydraulic motor on energy regenerative performance.

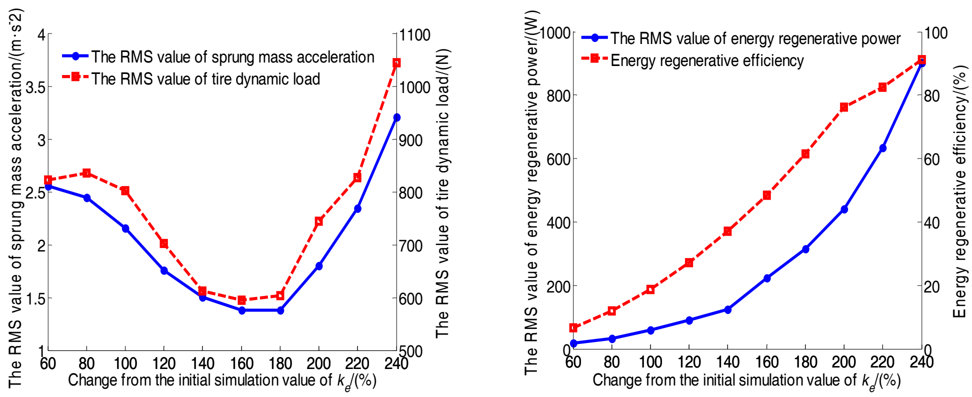


(**a**) (**b**)

**Figure 8.** Influence of the back electromotive force constant of the generator on evaluation indicators: (**a**) Influence of the back electromotive force constant of the generator on the damping performance; (**b**) Influence of the back electromotive force constant of the generator on energy regenerative performance.

Figure 6 shows that, firstly, with the increase of the effective area of hydraulic cylinder piston, the RMS value of the sprung mass acceleration and the dynamic load of the tire decrease gradually. Then they reach the minimum at nearly 1.2 times the value of original simulation parameters of the hydraulic cylinder piston effective area, which makes riding comfort continuously improve and the damping performance achieve optimal effect. Finally, with the increase of the effective area of hydraulic cylinder piston, the RMS value of the sprung mass acceleration and the dynamic load of the tire increase gradually, which leads to deterioration of ride comfort and the damping performance. However, with the increase of the effective area of hydraulic cylinder piston, the RMS value of energy regenerative power and energy regenerative efficiency increase gradually, that is to say, energy regenerative performance improves continuously. But when the RMS value of energy regenerative power and energy regenerative efficiency reach the maximum, which means energy regenerative efficiency is optimal, the RMS value of the sprung mass acceleration and the dynamic load of the tire reach the maximum too, which leads to the damping performance deterioration without meeting the design requirements of suspension.

Figure 7 shows that, firstly, with the increase of the displacement of the hydraulic motor, the RMS value of the sprung mass acceleration and the dynamic load of the tire decrease gradually. Then they reach the minimum at nearly 0.8 times the value of original simulation parameters of the displacement of the hydraulic motor, which makes riding comfort continuously improve and the damping performance achieve optimal effect. Finally, with the increase of the displacement of the hydraulic motor, the RMS value of the sprung mass acceleration and the dynamic load of the tire increase gradually, which leads to the deterioration of ride comfort and damping performance. However, with the increase of the displacement of the hydraulic motor, the RMS value of energy regenerative power and energy regenerative efficiency decrease gradually, that is to say, energy regenerative performance deteriorates continuously. But when the RMS value of energy regenerative power and energy regenerative efficiency reach the maximum, which means energy regenerative efficiency is optimal, the RMS value of the sprung mass acceleration and the dynamic load of the tire reach the maximum too, which leads to the damping performance deterioration, without meeting the design requirements of suspension.

Figure 8 simulation results show that, firstly, with the increase of back electromotive force constant of the generator, the RMS value of the sprung mass acceleration and the dynamic load of the tire decrease gradually. Then they reach the minimum at nearly 1.8 times the value of original simulation parameters of back electromotive force constant of the generator, which makes riding comfort continuously improve and the damping performance achieve optimal effect. Finally, with the increase of back electromotive force constant of the generator, the RMS value of the sprung mass acceleration and the dynamic load of the tire increase gradually, which leads to the deterioration of ride comfort and damping performance. However, with the increase of back electromotive force constant of the generator, the RMS value of energy regenerative power and energy regenerative efficiency increase gradually, that is to say, energy regenerative performance improves continuously. But when the RMS value of energy regenerative power and energy regenerative efficiency reach the maximum, which means energy regenerative efficiency is optimal, the RMS value of the sprung mass acceleration and the dynamic load of the tire reach the maximum too, which leads to the damping performance deterioration without meeting the design requirements of suspension.

From the above study, it can be concluded that with the change of parameters of EHA actuator, the damping performance and energy regenerative performance cannot achieve optimal effect at the same time, and there is the mutual restriction between them. In order to balance the damping performance and energy regenerative performance, the three main parameters of the EHA actuator, including the effective area of hydraulic cylinder piston $A$, the displacement of hydraulic motor $q$, and the back electromotive force constant of generator $k_e$, should be coordinated and optimized.

Peer-reviewed version available at Algorithms 2018, 11, 12; doi:10.3390/a11020012



*5.2. Optimization objectives and constraints*

In order to improve the energy regenerative performance under the requirement for meeting certain damping performance, genetic algorithm is used to optimize the parameters of the EHA actuator which can reduce the risk of being trapped in a locally optimal solution and make the optimization results more accurate[21-22].

The parameter optimization of semi-active energy regenerative suspension with EHA is a nonlinear optimization problem of single target and multi-variable. Taking energy regenerative power as the optimization goal, meeting certain damping performance as the constraint conditions, and taking the effective area of hydraulic cylinder piston $A$, displacement of the hydraulic motor $q$, and the back electromotive force constant of generator $k_e$ as optimization variables, genetic algorithm optimization toolbox from Matlab is used to optimize the parameters.

The objective function is the RMS value $\sigma_{Preg}$ of energy regenerative power of semi-active energy regenerative suspension with EHA, and $\sigma_{Preg}$ is given by:

$$\sigma_{Preg} = \sqrt{\frac{\sum_{i=1}^{N} Preg_i^2}{N}} \tag{29}$$

In the optimization toolbox, the objective function is required to minimize. In this paper however, the RMS value of energy regenerative power is required to maximize, so the method to minimize negative value of objective function is feasible.

The constraint condition in this paper is to meet certain damping performance. According to the automobile theory and other related literatures, the damping of vehicle suspension belongs to small damping, and the damping ratio $\xi$ meet the condition $0.2 \le \xi \le 0.4$. And when the RMS value of wheel dynamic load $\sigma_{F_d}$ does not exceed 1/3 of the static load value, the probability of wheel jumping off the ground is less than 0.15%, which can ensure the comfort and safety of suspension[23]. Meanwhile, the optimization toolbox requires that the constraint conditions are not positive. Thus the constraint conditions meet:

$$\begin{cases} 0.2 - \dfrac{c_s + c_{eq}(X)}{2\sqrt{k_s \cdot m_s}} \le 0 \\ \dfrac{c_s + c_{eq}(X)}{2\sqrt{k_s \cdot m_s}} - 0.4 \le 0 \\ \sigma_{F_d}(X) - \dfrac{1}{3}G \le 0 \end{cases} \tag{30}$$

where $X = \{x_1, x_2, x_3\} = \{A, q, k_e\}$ is optimal parameter vector.

*5.3. Optimization result analysis*

The above parameters are brought into the genetic algorithm optimization toolbox, and the optimization results of semi-active energy regenerative suspension with EHA are shown in table 1.

**Table 1.** Optimal parameters.

| **Optimal parameters** | **Symbol** | **Value** |
|---|---|---|
| The effective area of hydraulic cylinder piston | $A$ | 7.66e-4 $\mathrm{m}^2$ |
| The displacement of hydraulic motor | $q$ | 4.25 $\mathrm{mL/r}$ |
| The back electromotive force constant of generator | $k_e$ | 8.28e-3 $\mathrm{V \cdot min/r}$ |

Preprints (www.preprints.org) | NOT PEER-REVIEWED | Posted: 19 December 2017 doi:10.20944/preprints201712.0129.v1

Peer-reviewed version available at Algorithms 2018, 11, 12; doi:10.3390/a11020012



In order to verify the effect of the optimized EHA actuator parameters on the performances of semi-active energy regenerative suspension with EHA, the performance indexes of the suspension before and after optimization are simulated and compared assuming that the vehicle is traveling at the speed of 20m/s on the C grade road and the simulation time is 10s[24]. And the simulation results are shown in Table 2 and Figure 9 ~ Figure 11.

**Table 2.** Simulation results.

| Performance index | Symbol | Value | | Control effect / % |
|---|---|---|---|---|
| | | Before optimization | After optimization | |
| Sprung mass acceleration | $\sigma_a$ | 2.1585 $m/s^2$ | 1.7571 $m/s^2$ | -18.60 |
| Tire dynamic load | $\sigma_{Fd}$ | 802.7 N | 701.5 N | -12.61 |
| Energy regenerative power | $\sigma_{Preg}$ | 59.82 W | 89.53 W | 49.67 |
| Energy regenerative efficiency | $\eta$ | 18.68 % | 27.26 % | 45.93 |

Table 2 shows that after optimizing the parameters, the RMS value of sprung mass acceleration is reduced by 18.60%, which indicates that the ride comfort of vehicle has been improved to a certain extent, and the RMS value of tire dynamic load is decreased by 12.61%, which shows that vehicle driving safety has been enhanced, therefore the vehicle damping performance is improved. After the optimizing of parameters, the RMS value of energy regenerative power increases by 49.67%, and energy regenerative efficiency increases from 18.68% to 27.26%, which demonstrates that the vehicle energy regenerative performance was improved significantly.

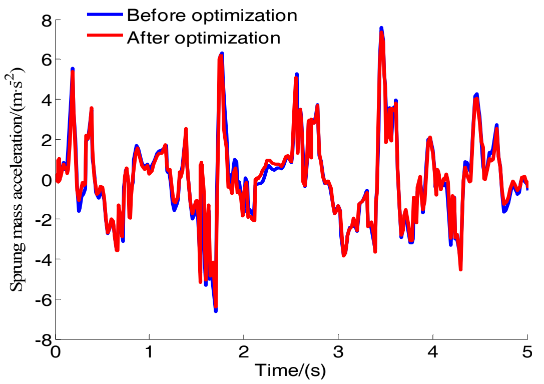


**Figure 9.** Spring mass acceleration response curve.

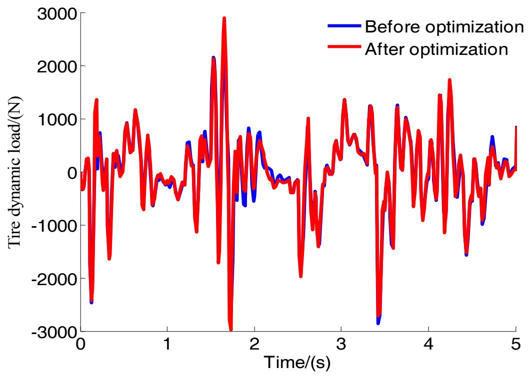


**Figure 10.** Tire dynamic load response curve.

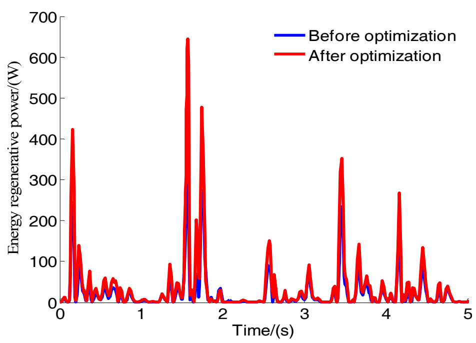


**Figure 11.** Energy regenerative power response curve.

Preprints (www.preprints.org) | NOT PEER-REVIEWED | Posted: 19 December 2017 doi:10.20944/preprints201712.0129.v1

Peer-reviewed version available at Algorithms 2018, 11, 12; doi:10.3390/a11020012



*5.4. Test and analysis*

In order to further verify the optimization results, EHA actuator prototype is redeveloped based on the optimization results, and the bench test is carried out as shown in Figure 12. In addition, the EHA actuator in Figure 4 is the original EHA actuator before optimization, and the EHA actuator in Figure 12 is the optimized one. Due to the limitation of test conditions, the test is conducted only for the spring mass acceleration and the energy regenerative power of semi-active suspension with EHA. In the test, the DH186 acceleration sensor produced by Donghua testing company is used to collect the spring mass acceleration signal, and the rectifier is used to rectify the three-phase alternating current generated by the DC brushless motor. At the same time, the Donghua DH5902 data acquisition system is used to collect the feed voltage signal. And according to the relationship between power, voltage and the internal resistance of the motor, the instantaneous energy regenerative power can be obtained. Under the condition that the sinusoidal is input at the frequency of 2Hz, the amplitude of 30mm and the sampling time of 10s, the test results of spring mass acceleration response and energy regenerative power response of semi-active suspension with EHA before and after optimization are shown in Figure 13 ~ Figure 14, respectively.

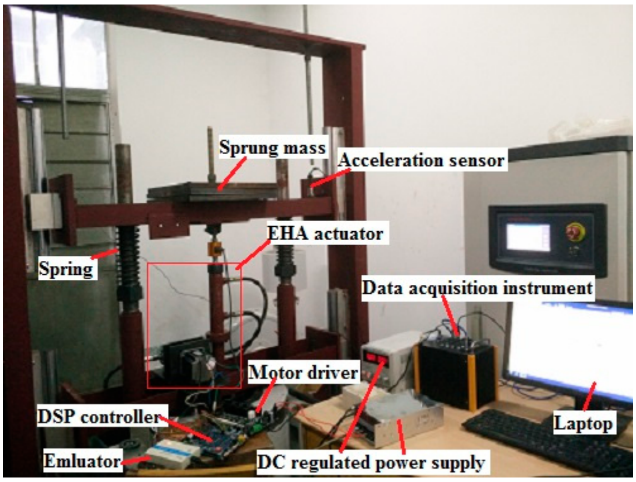


**Figure 12.** Bench test of EHA semi-active suspension system.

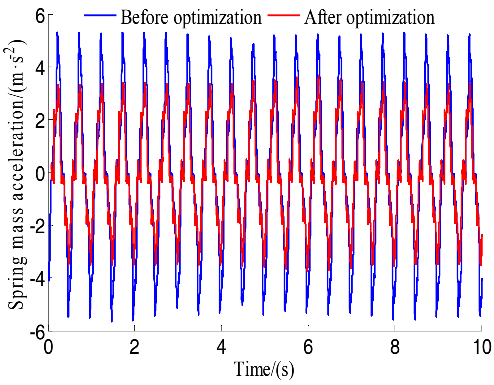


**Figure 13.** Test chart of spring mass acceleration response.

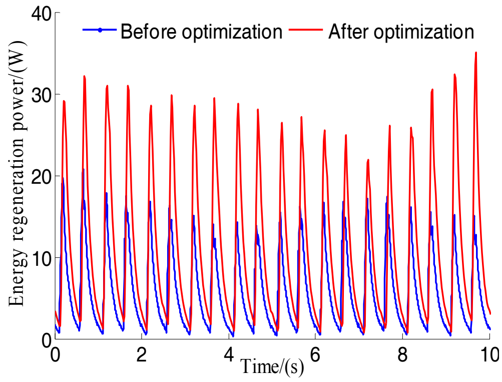


**Figure 14.** Test chart of energy regenerative power response.

## 6. Conclusions

In this paper, a structure of semi-active energy regenerative suspension with EHA is proposed. Following the proposed concept, a specific energy regenerative scheme and a composite energy recovery device are designed. On the basis of system structure, the physical prototypes are trial-manufactured, and the mechanical properties test of EHA semi-active suspension system are carried out. Based on the experimental data, the parameter identification for the system model is conducted via recursive least squares algorithm, which determines the equivalent spring stiffness $k_s$ and inherent damping coefficient of the system $c_s$. Moreover, the nonlinear model of the semi-active energy regenerative suspension with EHA is built.

On the basis of the nonlinear model, LQG control strategy of semi-active energy regenerative suspension with EHA is designed. And then a complete simulation model of the semi-active energy regenerative suspension with EHA is established in the Simulink.

In order to coordinate the damping performance and energy regenerative performance of semi-active energy regenerative suspension with EHA, the influences of the main parameters of EHA on the damping performance and energy regenerative performance of suspension are analyzed. Finally, the main parameters of EHA actuator are optimized using genetic algorithm.

In order to further verify the optimization results, EHA actuator prototype is redeveloped according to the optimization results, and the bench test is carried out. The test results show that when sinusoidal is input at the frequency of 2Hz and the amplitude of 30mm, the spring mass acceleration RMS value of optimized semi-active energy regenerative suspension with EHA is reduced by 22.23%, and the energy regenerative power RMS value is increased by 40.51%, which means under meeting the requirements of certain vehicle ride comfort and driving safety, the energy regenerative performance is improved significantly.

**Acknowledgments:** The authors gratefully acknowledge the support of National Natural Science Foundation of China (51775426, 51275403). Service Local Special Program Support Project of Shaanxi Provincial Education Department (17JF017) and Xi'an Science and Technology Project Funding Project (2017079CG/RC042-XAKD007). The authors would like to thank the anonymous reviewers for their valuable comments that significantly improved the quality of this paper.

**Conflicts of Interest:** The author declares that there is no conflict of interests regarding the publication of this paper.

## References

1. Tseng H. E.; Hrovat D. State of the art survey: active and semi-active suspension control. *Vehicle System Dynamics*. 2015, Volume 53, pp. 1034-1062.
2. Chen S. A; Li X.; Zhao L. J. Development of a control method for an electromagnetic semi-active suspension reclaiming energy with varying charge voltage in steps. *International Journal of Automotive Technology*. 2015, Volume 16, pp. 765-773.

3. Wu L. N.; Shi M. M.; Wang R. C. Parameter optimization of hybrid suspension with linear motor based on PSO. *Journal of Chongqing University of Technology(Natural Science)*. 2016, Volume 30, pp. 12-17.
4. Babak E.Development of Hybrid Electromagnetic Dampers for Vehicle Suspension Systems [D]. Canada: University of Waterloo，Waterloo，Ontario, 2009.
5. Okada Y.; Ozawa K. Energy Regenerative and Active Control of Electro-Dynamic Vibration Damper. *Transactions of the Japan Society of Mechanical Engineers C*, 2005, Volume 70, pp. 233-242.
6. Zhang H.; Guo X. X.; Hu S. B.; Fang Z. G.; Xu L. Simulation analysis on hydraulic-electrical energy regenerative semi-active suspension control characteristic and energy recovery validation test. *Transactions of the Chinese Society of Agricultural Engineering(Transactions of the CSAE*. 2017, Volume 33, pp. 64-71.
7. Efatpenah F.; Beno J. H.; Weeks D. A. Energy requirements of a passive and an electromechanical active suspension system. *Vehicle System Dynamics*. 2000, Volume 34, pp. 437-458.
8. Goldner R.; Zerigian P.; Hull J. A preliminary study of energy recovery in vehicles by using Regenerative magnetic shock absorbers. *SAE Paper*. 2001, pp. 2001-2011.
9. Zuo L.; Nayfeh S. A. Structured H2 optimization of vehicle suspensions based on multi-wheel models. *Veh. Syst. Dyn*. 2003, Volume 40, pp. 351–371.
10. Anubi O. M.; Clemen L. Energy-regenerative model predictive control. *J. Franklin Inst.* 2015, Volume 352, pp. 2152–2170.
11. Clemen L.; Margolis D. Modeling and control of a quarter car electrodynamic air-suspension. *International Conference on Bond Graph Modeling, Monterey, CA*. 2014, pp. 27–33.
12. Zuo L.; Scully B.; Shestani J.; Zhou Y. Design and characterization of an electromagnetic energy harvester for vehicle suspensions. *Smart Material and Structure*. 2010, Volume 19, pp. 145-153.
13. Zuo L., Tang X. D. Large-scale vibration energy harvesting. *Journal of Intelligent Material Systems and Structure*. 2013, Volume 24, pp. 1405-1430.
14. Huang K.; Zhang Y. C.; Yu F. Coordinate optimization for synthetical performance of electrical energy-regenerative active suspension. *Journal of Shanghai Jiao tong University*. 2009, Volume 43, pp. 226-230.
15. Wang Q. N., Liu S. S.; Wang W. H. Structure design and parameter matching of ball-screw regenerative damper. *Journal of Jilin University Engineering and Technology*. 2012, Volume 42, pp. 1100-1106.
16. Kou F. R. Design and energy regenerative study on semi-active suspension with electro-hydrostatic actuator. *Transactions of the Chinese Society for Agricultural Machinery*. 2016, Volume 28, pp. 352-359.
17. Martins I.; Estevez J.; Marques G. Permanent-magnets linear actuators applicability in automobile active suspensions. *IEEE Transactions on Vehicular Technology*. 2006, Volume 55, pp. 86-94.
18. Kou F. R.; Fan Y. Q.; Zhang C. W.;Du J. F.; Wang Z. Time delay compensation control of semi-active suspension with vehicle electro-hydrostatic actuator. *China Mechanical Engineering*. 2016, Volume 27, pp. 2111-2117.
19. Sun X. Q.; Chen L.; Wang S. H. Nonlinear modeling and parameter optimization of two-stage series-connected ISD suspension. *Transactions of the Chinese Society for Agricultural Machinery*. 2014, Volume 45, pp. 7-13.
20. Kawamoto Y.; Suda Y.; Inoue H. Electro-mechanical suspension system considering energy consumption and vehicle manoeuvre.*Vehicle System Dynamics*. 2008, Volume 46, pp. 1053-1063.
21. Kou F. R.; Du J. F.; Zhang C. W.; Wang Y. J.; Wang Y. Z. Multi-mode switching control of self-powered active suspension with electro-hydrostatic actuator. *Mechanical Science and Technology for Aerospace Engineering*. 2016, Volume 35, pp. 1937-1943.
22. Li C.; Zhu R. R.; Liang M. Integration of shock absorption and energy harvesting using a hydraulic rectifier. *Journal of Sound and Vibration*. 2014, Volume 33, no. 17, pp. 3904-3916.
23. Zhao L. F.; Hu J. F.; Zhang R. Y. Integrated optimization design of cab suspension and suspension parameters for heavy tractor. *China Mechanical Engineering*, 2016, Volume 27, pp. 791-808.
24. Zhan M. Dynamic simulation and performance study of hydraulic electromagnetic regenerative shock absorber. Jilin University, ChangChun, 2015.